Aust. J. Phys., 1986, 39, 667–78

Inclusion of Relativistic Effects in Electronic Structure Calculations*

K. G. Dyall

Department of Chemistry, Monash University, Clayton, Vic. 3168.

Abstract

The effects of relativity on atomic and molecular structure are discussed with an indication of their importance as a function of atomic number. Perturbation methods for the inclusion of relativistic effects are briefly analysed in terms of the Dirac equation; the multi-configuration Dirac–Fock method for the variational treatment of relativistic effects is then discussed in more detail. Finally, a case study on 2p ionisation in Ca is presented, in which higher-order relativistic effects are important.

1. Introduction

There has been a great deal of attention paid recently to the inclusion of relativistic effects in electronic structure calculations on atoms and molecules, by use of the Dirac equation. It has been the subject of a number of reviews (Pyykkö 1978; Pyykkö and Desclaux 1979; Pitzer 1979; McKelvey 1983) and workshops (Malli 1983; see also *Int. J. Quantum Chem.*, Vol. 24), and has even made its way into undergraduate courses (Banna 1985). In this paper, material from several sources is gathered with work of the author to discuss the effects of relativity on structure and the circumstances under which relativistic effects must be included in electronic structure calculations by other than perturbative methods.

The first consideration in the incorporation of relativistic effects is in some ways a practical one: we ask, for what purpose does one wish to include them. Experience with atomic structure has shown that calculations which proceed from a fully relativistic model take more than twice as long as the corresponding nonrelativistic calculations. It is therefore necessary to ascertain what level of accuracy is required, and therefore whether inclusion of relativistic effects in themselves makes a significant difference to the results, or whether the error in including them by perturbation theory is significant. For example, calculations for order-of-magnitude estimates of a quantity may not need to consider relativity at all, whereas calculations of experimental accuracy on the hydrogen atom must account for relativistic effects in detail. In making an assessment of whether relativistic effects should be included, and by what means, it is useful to have an overview of the effect of relativity on structure, the size of relativistic effects in the periodic system and some criteria for judging their importance.

* Paper presented at the Specialist Workshop on Excited and Ionised States of Atoms and Molecules, Strathgordon, Tasmania, 3–7 February 1986.

0004-9506/86/050667$02.00

2. Effects of Relativity on Structure

(a) Direct Effects: One-electron Atoms

The first effect of relativity on atomic structure can be demonstrated simply, without reference to relativistic quantum mechanics. The theory of relativity relates changes in various properties of a particle to its speed v, relative to the speed of light c. For example, the mass m of the particle is related to its rest mass m_0 by

$$m = \frac{m_0}{\sqrt{(1 - v^2/c^2)}}. \tag{1}$$

Since v^2 must always be greater than or equal to zero, the mass of the moving particle will always be greater than the rest mass. The mass of the electron appears in the denominator of the expression for the Bohr radius:

$$a_0 = h^2/4\pi^2 me^4$$

and, from above, the mass of the electron will be greater than its rest mass. Thus the direct effect of relativity is to *contract* the atomic orbitals.

The size of this contraction and its effect on the energy can also be demonstrated simply. From a nonrelativistic model of atomic structure, the average squared velocity of an electron in a hydrogenic orbital is related to the nuclear charge Z and the principal quantum number of the orbital n (in Hartree atomic units) by

$$\langle v^2 \rangle = Z^2/n^2. \tag{2}$$

If the criterion for the inclusion of relativistic effects in a structure model was a change of 5% in the mass and hence in the orbital mean radius, then $\langle v^2 \rangle = 0{\cdot}1c^2$, and the corresponding value of Z/n is 43. If the criterion was a change of 0·5% in the mass, then $\langle v^2 \rangle = 0{\cdot}01c^2$, giving $Z/n = 14$. With the first criterion, one would not need to include relativistic effects for the 1s orbital until the 4d block, but with the second criterion, it would be necessary for the 3p block. The corresponding changes in the orbital energy can be found by expanding the Sommerfeld eigenvalue expression in powers of Z^2/c^2:

$$\epsilon_{1s} = -\tfrac{1}{2}Z^2(1 + \tfrac{1}{4}Z^2/c^2 + \ldots). \tag{3}$$

For a 5% change in the eigenvalue, $Z^2 = 0{\cdot}2c^2$, or $Z = 61$; for a change of 0·5%, $Z = 19$.

Another criterion which could be applied to determine whether relativistic effects need to be included is the probability that an electron will be moving at a greater fraction of the speed of light than some selected value. This will occur when the electron is closer to the nucleus than a given distance, which will depend on the atomic number. Fig. 1 shows this probability for a 1s electron travelling faster than $0{\cdot}3c$, as a function of atomic number.

The second effect of relativity on atomic structure does require a consideration of the relativistic theory. Nonrelativistic quantum mechanics does not implicitly include the spin angular momentum of the particles in the system—it is tacked on, almost as an afterthought. Relativistic quantum mechanics includes it from the beginning, coupled to the orbital angular momentum to produce a total angular momentum.

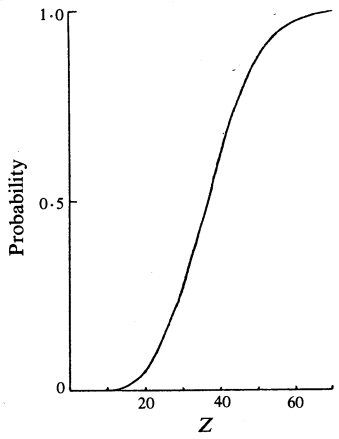

Fig. 1. Probability of finding a 1s electron within a radius of $10^{-3}Z$ a.u., as a function of atomic number Z.

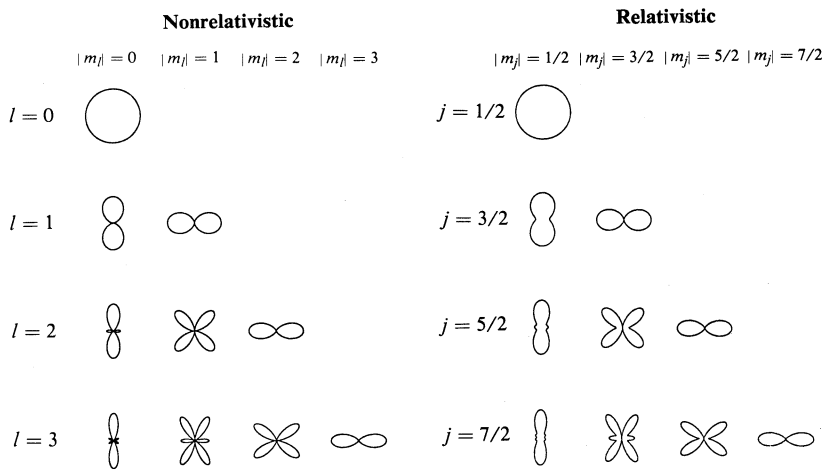

Fig. 2. Polar diagrams of squared angular wavefunctions ('orbital shapes').

The value of the spin quantum number for the electron, $\frac{1}{2}$, gives rise to *two* values of the total angular momentum j for each orbital with $l > 0$. Thus each nonrelativistic orbital is split into two relativistic orbitals,* characterised by their total angular momentum. It is worth noting that the angular distributions ('shapes') of these relativistic orbitals are determined by the value of j and not that of l (see Fig. 2).

* The word 'orbital' is used here to denote a set of wavefunctions with a common radial function.

Relativistic theory also changes the nature of the wavefunction. The Schrödinger equation has a scalar solution. The relativistic equivalent, the Dirac–Coulomb equation, has a four-component vector as its solution,

$$\psi = \begin{bmatrix} \psi_1 \\ \psi_2 \\ \psi_3 \\ \psi_4 \end{bmatrix} = \begin{bmatrix} \psi^{\mathrm{L}} \\ \psi^{\mathrm{S}} \end{bmatrix}, \tag{4}$$

which is partitioned into two two-component vectors, a 'large' component ψ^{L} and a 'small' component ψ^{S}, so-called because for most structure calculations the large component describes most of the electron density. The components of the large and small component vectors can be described as 'spin-up' (ψ_1 and ψ_3) and 'spin-down' (ψ_2 and ψ_4).

Table 1. Effect of core potential and valence dynamics on valence orbital eigenvalues for selected heavy elements

All values are in eV; the top row of headings refers to the potential, the bottom row to the dynamics

Heavy element	Orbital eigenvalue	Rel. Rel.	Nonrel. Rel.	Nonrel. Nonrel.	Rel. Nonrel.
Au	ϵ_{6s}	7·94	7·97	6·01	6·18
Tl	$\epsilon_{6\bar{p}}$	5·81	6·79	5·24	4·58
	ϵ_{6p}	4·79	5·63	5·24	4·46
Lu	$\epsilon_{6\bar{d}}$	5·25	7·32	6·63	4·74
	ϵ_{6d}	5·01	6·90	6·63	4·81

(b) Indirect Effects: Many Electron Atoms

The direct effects of relativity on structure discussed in the preceding subsection are the primary effects on structure; but in addition to these are secondary effects which arise as a consequence of the operation of the primary effects in a many-electron environment. From the above considerations, relativity will be most important for core orbitals, which have a high *effective* charge and small principal quantum number. Since their behaviour is dominated by the presence of the nuclear potential and are therefore most nearly hydrogenic, they will contract. The effect of this contraction on the outer orbitals is to screen them more effectively. These may either contract or expand, depending on the balance between the increased screening and the relativistic contraction. Rose *et al.* (1978) have assessed the importance of screening against direct effects in a series of calculations on atoms with a single electron outside a closed shell. Essentially, the valence electron is treated as a single particle moving in a potential which can be constructed from nonrelativistic or relativistic wavefunctions. The wavefunction for the electron is then determined using either the Schrödinger equation or the Dirac equation, i.e., using nonrelativistic or relativistic dynamics. The results are reproduced in Table 1. For the 6s electron, the effect of the core potential is minimal. This is explained by the penetration of the core by the 6s wavefunction. For the $6\bar{p}$ orbital, the direct effect is also important, since the small component of

this orbital has s-character, and therefore penetrates to the nucleus. The direct and indirect effects nearly cancel, making the $6\bar{p}$ orbital a little more contracted than the nonrelativistic 6p orbital. The 6p orbital expands slightly, since its small component is d-like. For the 6d orbital, the screening effects are dominant, though it is clear that there is still a relativistic concentration. These calculations make it clear that relativistic effects may have to be incorporated even in the valence shell, in contrast to the predictions of the simple hydrogenic approach.

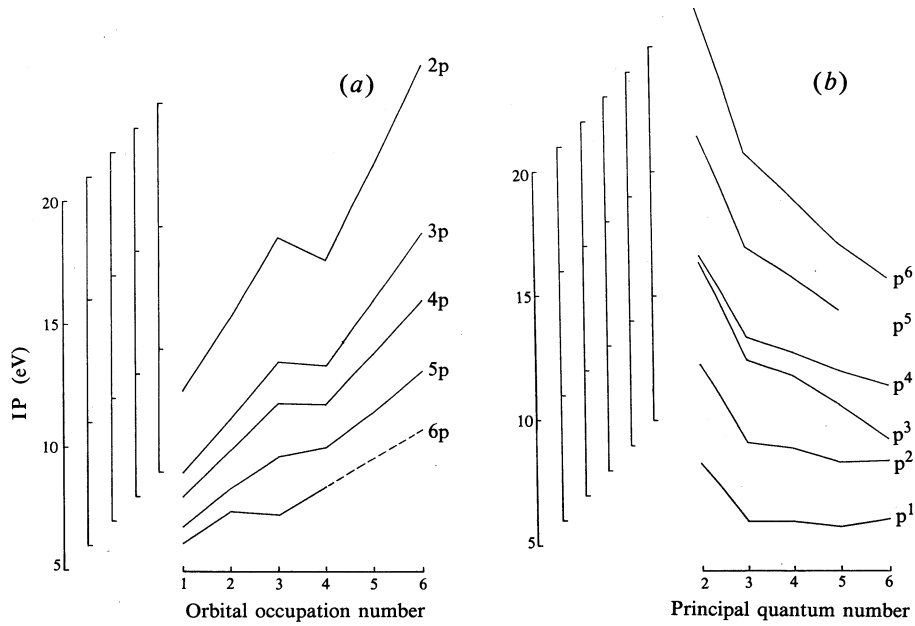

Fig. 3. Experimental first ionisation potentials of p-block elements, displayed as a function of (*a*) orbital occupation number for each period and (*b*) principal quantum number for each group.

The importance of relativistic effects in the valence shell of the heavy elements can be demonstrated by the trends in the experimental ionisation potentials (IP). Fig. 3*a* displays the first ionisation potentials of the p-block elements as a function of orbital occupation number for each period. The trend expected on the basis of a nonrelativistic model, in which the IP increases across the period due to imperfect screening, and decreases when it is first necessary to pair two electrons, is clearly seen for the 2p, 3p and 4p elements. For the 5p elements, the difference in IP between p^1 and p^2 is greater than the difference in IP between p^2 and p^3, in contrast to the previous periods, while for the 6p elements, there is a definite decrease in IP from p^2 to p^3. Examining the trends down the groups (Fig. 3*b*), it is clear that the p^1 and p^2 elements show different behaviour from the rest: the IP increases from $n = 5$ to $n = 6$. Evidently, the 6p subshell must be treated relativistically, since the splitting between the $6\bar{p}$ and 6p orbital is large enough to substantially affect the energies. Similar conclusions could be drawn from the electron affinities of the Group 1 elements, the ionisation potentials of the elements in Groups 1 and 2 and other properties.

Table 2. Overlap integrals between nonrelativistic and relativistic radial functions P, and between spin–orbit components of relativisitic p radial functions, for the Group 4 elements

Element	n	$\langle P^{NR}_{ns} \mid P^{R}_{ns} \rangle$	$\langle P^{NR}_{np} \mid P^{R}_{n\bar{p}} \rangle$	$\langle P^{NR}_{np} \mid P^{R}_{np} \rangle$	$\langle P_{n\bar{p}} \mid P_{np} \rangle$
C	2	0·999572	0·999967	0·999967	0·999967
Si	3	0·999974	0·999985	0·999987	0·999987
Ge	4	0·999648	0·999807	0·999974	0·999738
Sn	5	0·997675	0·998558	0·999938	0·998320
Pb	6	0·975646	0·982948	0·999542	0·981497

Table 3. Contribution to electron density of small components for valence shells of Group 4 elements

Values have been multiplied by 10^6

Element	n	ns	$n\bar{p}$	np
C	2	41	33	33
Si	3	37	25	25
Ge	4	55	32	31
Sn	5	62	36	33
Pb	6	91	52	38

Table 4. Percentage contribution to electron density of small components for all orbitals of Pb

Orbital	Value	Orbital	Value
1s	9·7819	$4\bar{d}$	0·2017
2s	2·2586	4d	0·1940
$2\bar{p}$	2·2635	$4\bar{f}$	0·1572
2p	1·9923	4f	0·1541
3s	0·7617	5s	0·0663
$3\bar{p}$	0·7548	$5\bar{p}$	0·0582
3p	0·6771	5p	0·0496
$3\bar{d}$	0·6627	$5\bar{d}$	0·0324
3d	0·6417	5d	0·0301
4s	0·2595	6s	0·0091
$4\bar{p}$	0·2499	$6\bar{p}$	0·0052
4p	0·2225	6p	0·0038

Table 5. Composition of lowest $J = 0$ eigenvector in LS and jj coupling for the Group 4 elements

Element	n	Weights of LS CSF		Weights of jj CSF	
		$\mid np^2\ {}^3P_0\rangle$	$\mid np^2\ {}^1S_0\rangle$	$\mid n\bar{p}^2\ J = 0\rangle$	$\mid np^2\ J = 0\rangle$
		1·000000[A]	0·000000[A]	0·666667[A]	0·333333[A]
C	2	0·999997	0·000003	0·668252	0·331748
Si	3	0·999903	0·000097	0·675908	0·324092
Ge	4	0·996877	0·003123	0·718230	0·281770
Sn	5	0·981042	0·018958	0·788923	0·211077
Pb	6	0·889736	0·110264	0·925217	0·074783
		0·666667[B]	0·333333[B]	1·000000[B]	0·000000[B]

[A] Nonrelativistic limit. [B] Relativistic limit.

There are several other criteria which could be applied to determine the importance of relativistic effects, which relate to the change in the radial wavefunctions from the nonrelativistic wavefunctions. The first is the overlap between the large component radial function and the nonrelativistic radial function to which it reduces in the limit $c \rightarrow \infty$; the second is the overlap between the $j = l-\frac{1}{2}$ and $j = l+\frac{1}{2}$ large components; and the third is the partitioning of the electron density between the large and small components. Table 2 gives the valence orbital overlaps and Table 3 the partitioning for the Group 4 elements. The principal effect in the valence shell is the change in the large component function: the small component contributes very little to the total electron density. Table 4 gives the partitioning for all orbitals of Pb. We note that the small component contribution to the electron density is nearly 10% for the 1s orbital, but is only 0·01% for the 6s orbital. The effect of relativity could also be assessed in terms of the deviation of the atomic state functions (ASF) from *LS* coupling. For example, the lowest $J = 0$ state can be expressed in terms of the two *jj* coupled configuration state functions (CSF) $|n\bar{p}^2\ J = 0\rangle$ and $|np^2\ J = 0\rangle$, or in terms of the *LS* coupled CSF $|np^2\ {}^3P_0\rangle$ and $|np^2\ {}^1S_0\rangle$. At the nonrelativistic limit, the ASF will be the pure *LS* coupled $|np^2\ {}^3P_0\rangle$; in the relativistic limit, it will be the pure *jj* coupled $|n\bar{p}^2\ J = 0\rangle$. Table 5 gives the eigenvector composition of this state for the Group 4 elements.

(c) Effects on Bonding in Molecules

The direct and indirect effects discussed in the previous subsections apply to molecules as well, but to them must be added some considerations of the effects of relativity on bonding. The common model of bonding is that of a diatomic molecule, in which the molecular orbitals are formed from a linear combination of atomic orbitals. Within a relativistic framework, the spin coupling will mix orbitals of different nonrelativistic symmetry types. In Table 6, the various combinations of relativistic s and p atomic orbitals to form molecular orbitals are shown. We note that for $m_j = j$, the orbitals are pure bonding or pure antibonding, but for the rest, there is a mixture of bonding and antibonding or nonbonding character. In particular, relativistic $p\sigma$ orbitals will be weaker than expected due to admixture of $p\pi^*$ antibonding character; $p\pi_{1/2}$ orbitals will be similarly weakened by admixture of $p\sigma^*_{1/2}$ antibonding character. Hybrid $sp^n\sigma$ orbitals will also be slightly weaker due to the nonbonding character from the relativistic p orbital. Because of the closeness of the $\bar{p}$ and p orbitals, there will be considerable mixing of the $\bar{p}\sigma_{1/2}$ and $p\sigma_{1/2}$ orbitals, so that for light atoms the orbital will be nearly pure σ bonding. For heavy elements, where the spin–orbit splitting is large, there will be significant π^* character in the orbital, which will manifest itself in the weakness of the bond. An example of relativistic p bonding is Tl_2, which is weakly bound: its dissociation energy is not accurately determined, but is about 0·6 eV (see Pitzer 1979 for further discussion).

3. Methods for the Inclusion of Relativistic Effects

(a) Perturbation Methods

The most common method for the inclusion of relativistic effects in structure calculations is the perturbation method, based on nonrelativistic wavefunctions. The perturbation Hamiltonian can be derived from the Dirac equation as follows. By

Table 6. Combination of relativistic s and p atomic 2-spinors to form molecular spinors
The molecular axis is taken to be the z axis. Orbital types only are given: normalisation is not included. Subscripts in labels indicate m_j quantum number; spinors are only shown for positive m_j; 'A+B' and 'A−B' indicate in-phase and out-of-phase combinations of atomic spinors to form molecular spinors

Atom A		Atom B		Molecule (A+B)		Molecule (A−B)	
Label	Spinor	Label	Spinor	Label	Spinor	Label	Spinor
$s_{1/2}$	$\begin{bmatrix} s \\ 0 \end{bmatrix}$	$s_{1/2}$	$\begin{bmatrix} s \\ 0 \end{bmatrix}$	$s\sigma_{1/2g}$	$\begin{bmatrix} s\sigma \\ 0 \end{bmatrix}$	$s\sigma_{1/2u}$	$\begin{bmatrix} s\sigma^* \\ 0 \end{bmatrix}$
$s_{1/2}$	$\begin{bmatrix} s \\ 0 \end{bmatrix}$	$\bar{p}_{1/2}$	$\begin{bmatrix} -p_0 \\ p_1 \end{bmatrix}$	$sp\sigma^*_{1/2}$	$\begin{bmatrix} sp\sigma^* \\ n_p \end{bmatrix}$	$sp\sigma_{1/2}$	$\begin{bmatrix} sp\sigma \\ -n_p \end{bmatrix}$
$s_{1/2}$	$\begin{bmatrix} s \\ 0 \end{bmatrix}$	$p_{1/2}$	$\begin{bmatrix} p_0 \\ p_1 \end{bmatrix}$	$sp\sigma_{1/2}$	$\begin{bmatrix} sp\sigma \\ n_p \end{bmatrix}$	$sp\sigma^*_{1/2}$	$\begin{bmatrix} sp\sigma^* \\ -n_p \end{bmatrix}$
$\bar{p}_{1/2}$	$\begin{bmatrix} -p_0 \\ p_1 \end{bmatrix}$	$\bar{p}_{1/2}$	$\begin{bmatrix} -p_0 \\ p_1 \end{bmatrix}$	$p\pi_{1/2u}$	$\begin{bmatrix} -p\sigma^* \\ p\pi \end{bmatrix}$	$p\pi_{1/2g}$	$\begin{bmatrix} -p\sigma \\ p\pi^* \end{bmatrix}$
$\bar{p}_{1/2}$	$\begin{bmatrix} -p_0 \\ p_1 \end{bmatrix}$	$p_{1/2}$	$\begin{bmatrix} p_0 \\ p_1 \end{bmatrix}$	—	$\begin{bmatrix} -p\sigma \\ p\pi \end{bmatrix}$	—	$\begin{bmatrix} -p\sigma^* \\ p\pi^* \end{bmatrix}$
$p_{1/2}$	$\begin{bmatrix} p_0 \\ p_1 \end{bmatrix}$	$p_{1/2}$	$\begin{bmatrix} p_0 \\ p_1 \end{bmatrix}$	$p\sigma_{1/2u}$	$\begin{bmatrix} p\sigma^* \\ p\pi \end{bmatrix}$	$p\sigma_{1/2g}$	$\begin{bmatrix} p\sigma \\ p\pi^* \end{bmatrix}$
$p_{3/2}$	$\begin{bmatrix} p_1 \\ 0 \end{bmatrix}$	$p_{3/2}$	$\begin{bmatrix} p_1 \\ 0 \end{bmatrix}$	$p\pi_{3/2u}$	$\begin{bmatrix} p\pi \\ 0 \end{bmatrix}$	$p\pi_{3/2g}$	$\begin{bmatrix} p\pi^* \\ 0 \end{bmatrix}$

writing the Dirac equation as a matrix equation in terms of the large and small components,

$$\begin{bmatrix} VI_2 & c\boldsymbol{\sigma}.\boldsymbol{p} \\ c\boldsymbol{\sigma}.\boldsymbol{p} & (V-2c^2)I_2 \end{bmatrix} \begin{bmatrix} \psi^{\mathrm{L}} \\ \psi^{\mathrm{S}} \end{bmatrix} = \epsilon \begin{bmatrix} \psi^{\mathrm{L}} \\ \psi^{\mathrm{S}} \end{bmatrix}, \tag{5}$$

where I_2 is the 2×2 unit matrix and $\boldsymbol{\sigma} = (\sigma_x, \sigma_y, \sigma_z)$ is the vector of Pauli spin matrices, the small component of the Dirac wavefunction is eliminated to give an equation involving only the large component

$$V\psi^{\mathrm{L}} + \tfrac{1}{2}(\boldsymbol{\sigma}.\boldsymbol{p})\{1-(V-\epsilon)/2c^2\}^{-1}(\boldsymbol{\sigma}.\boldsymbol{p})\psi^{\mathrm{L}} = \epsilon\psi^{\mathrm{L}}, \tag{6a}$$

and the denominator in the second term of this expression is expanded in powers of α^2 (i.e. $1/c^2$), the perturbation parameter:

$$\{VI_2 + \tfrac{1}{2}(\boldsymbol{\sigma}.\boldsymbol{p})(\boldsymbol{\sigma}.\boldsymbol{p}) + \tfrac{1}{4}\alpha^2(\boldsymbol{\sigma}.\boldsymbol{p})(V-\epsilon)(\boldsymbol{\sigma}.\boldsymbol{p}) + \ldots\}\psi^{\mathrm{L}} = \epsilon\psi^{\mathrm{L}}. \tag{6b}$$

From the properties of the spin matrices, it is easy to show that the second term in the braces is equivalent to the Schrödinger kinetic energy operator $-\frac{1}{2}\nabla^2 I_2$. The third term is the lowest order relativistic correction to the Schrödinger Hamiltonian. Truncation of the perturbation Hamiltonian is usually made after the term in α^2, but does not always include all the effects of order α^2. We note that the potential V may also include relativistic corrections (e.g. the Breit interaction) which may have to be included in the perturbation Hamiltonian, or in the elimination of the small component. The zero-order wavefunction is simply the Schrödinger wavefunction.

(b) Multi-configurational Dirac–Fock (MCDF) Method

The MCDF method has been discussed in detail by a number of authors (Desclaux 1975; Grant *et al.* 1980 and references therein; Froese Fischer 1977); the foundations of relativistic self-consistent field theory have been discussed by Grant (1986, present issue p. 649). Here it is sufficient to discuss the multi-configuration method and its use within various approximations.

We start with an energy functional E, which is represented as a (statistically) weighted sum of energies of atomic states E_n,

$$E = \sum_n (2J_n+1)E_n . \tag{7}$$

The ASF Ψ_n are written as a linear combination of CSF Φ_i,

$$\Psi_n = \sum_i c_{ni}\,\Phi_i , \tag{8}$$

from which the energies E_n can be derived:

$$E_n = \sum_{i,j} c^\dagger_{in}\, c_{nj}\, H_{ij}; \qquad H_{ij} = \langle \Phi_i | \hat{H} | \Phi_j \rangle . \tag{9}$$

Thus the energy functional can be written

$$E = \sum_{i,j} H_{ij} \sum_n (2J_n+1) c^\dagger_{in}\, c_{nj} . \tag{10}$$

Three kinds of multi-configuration methods can now be identified. The first method is the 'true' multi-configuration self-consistent field (MCSCF) method, in which the energy of only *one* ASF is determined, i.e. the sum over n is limited to one member. This is called the MCDF-OL method by Grant *et al.* (1980). In the second method, the sum over n is restricted to a few members, giving the best energies for a group of states, i.e. a multi-reference MCSCF method, called the MCDF-EOL method by Grant *et al.* The third method includes all ASF in the sum. From closure, we write

$$\sum_n (2J_n+1) c^\dagger_{in}\, c_{nj} = (2J_i+1)\delta_{ij} , \tag{11}$$

so that the energy functional reduces to

$$E = \sum_i (2J_i+1) H_{ii} , \tag{12}$$

which no longer contains the coefficients. This is called the MCDF-EAL method, or MCDF-AL if there is only one value of the total angular momentum. There is

no important distinction between the AL and EAL methods. Thus, the OL and EOL methods both involve the variation of the energy functional with respect to the one-electron functions which compose the CSF and the CSF mixing coefficients, whereas the (E)AL method only requires the variation of the one-electron functions.

(c) Use of the Methods

The advantage of the perturbation methods is that they require less computation than the Dirac equation, principally because they use the Schrödinger wavefunctions. It is also possible with the perturbation methods to include all contributions of a particular order in α^2. Thus, perturbation methods are satisfactory for most problems involving light elements and outer shells, but when there is significant change in the wavefunctions due to relativistic effects, the Dirac equation must be used to obtain wavefunctions. With the Coulomb interaction only included in the potential, the Dirac wavefunctions and energies include some, but not all, of the relativistic effects to all orders in α^2. The remaining effects must be obtained by the inclusion of the full transverse photon interaction in the potential and incorporation of quantum electrodynamics (QED). The transverse interaction is usually added as a perturbation after the determination of the Dirac–Coulomb wavefunctions, along with the lowest order QED effects, i.e. self-energy and vacuum polarisation (McKenzie *et al.* 1980). While the second- and fourth-order vacuum polarisation potentials can be calculated with reasonable accuracy, the self-energy must be estimated by a rather crude screening method from values for one-electron ions, although there has been a move recently to develop methods for calculation of the self-energy for non-hydrogenic wavefunctions (Weitsman and Hagelstein 1986). Nevertheless, the current methods give reasonably accurate fine structure intervals. For example, the predicted (single-configuration) splitting of the $^2P_{3/2}$ and $^2P_{1/2}$ levels of the [3p] configuration in Ar^+ is 1446 cm^{-1}, compared with the experimental value of 1432 cm^{-1}, an accuracy of 1%. The corresponding values for the [5p] configuration of Xe^+ are 10592 cm^{-1} and 10537 cm^{-1}, an accuracy of 0·5%.

The inclusion of higher-order effects may also be important where there are near-degeneracies in the atomic states. From second-order perturbation theory we write

$$E^{(2)} = \sum_n \frac{|H_{0n}|^2}{E_n - E_0}. \tag{13}$$

The second-order energy may be large if there is a small energy difference between the basis states, even if the matrix elements connecting them are small. Thus, higher-order relativistic effects can have a large effect on a system, even if they do not contribute much to the total energy, or the relative energies of the states of the system. In the next section, a case study will be presented in which the importance of near-degeneracy and the inclusion of higher-order effects is displayed.

4. Case Study: Ionisation of the 2p Subshell in Atomic Calcium

The history of this study commenced with the observation of an anomaly in the ratios of the intensities of L_3–MM to L_2–MM Auger lines in the series Ar, K, Ca (Breuckmann 1978). For Ar and K, the $L_3 : L_2$ ratios were close to the statistical 2 : 1 value, but for Ca, the ratio was 0·9 : 1. The Auger transitions in Ca were accompanied by a much more intense group of satellites than in Ar or K. It was

thought that this phenomenon was related to the collapse of the 3d orbital as the first transition series was approached: core-ionised calcium should behave much like scandium. The MCHF calculations on the 2p hole state which included the CSF* $|(\text{Ar[2p]})4s^2\ ^2\text{P}\rangle$ and $|(\text{Ar[2p]})3d^2\ ^1\text{S}\ ^2\text{P}\rangle$ showed that there was indeed a collapse of the 3d orbital, causing strong mixing of these two CSF in the ASF. This, however, could not explain the anomalous $L_3 : L_2$ ratio. Calculations were therefore undertaken with the MCDF programs (Grant *et al.* 1980; McKenzie *et al.* 1980) to determine whether there was some J-dependent mixing of CSF. Results have been reported by Weber *et al.* 1983.

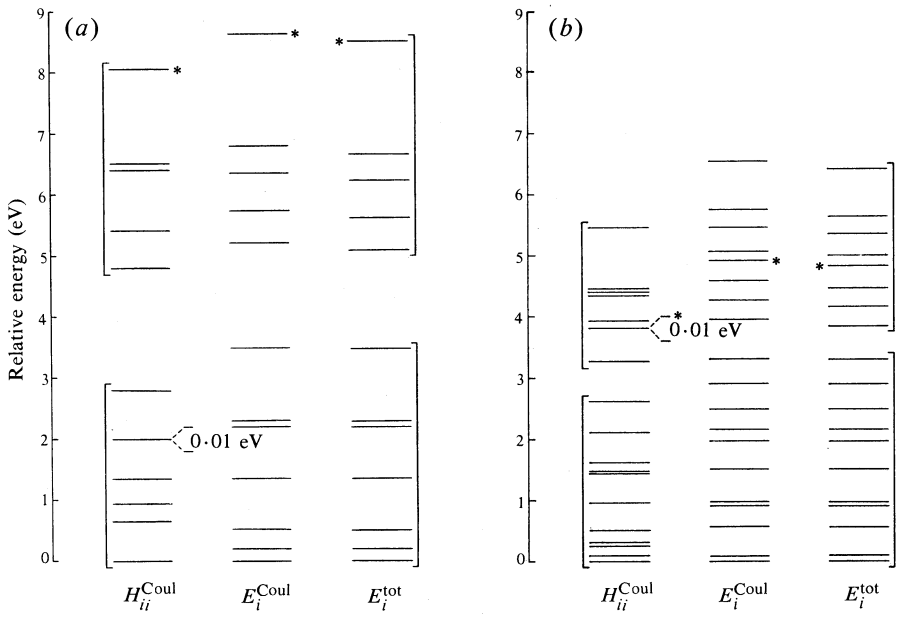

Fig. 4. Diagram of energy levels of (*a*) $J = \frac{1}{2}$ and (*b*) $J = \frac{3}{2}$ CSF and ASF (with and without higher-order corrections) from the configurations $(\text{Ar[2p]})4s^2$, $(\text{Ar[2p]})4s3d$ and $(\text{Ar[2p]})3d^2$ of the calcium atom. The levels marked with an asterisk are those assigned to the $(\text{Ar[2p]})4s^2$ configuration. The brackets indicate grouping of energy levels according to the core hole, i.e. $[2\bar{p}]$ or [2p].

The calculations took the CSF from the configurations $(\text{Ar[2p]})4s^2$, $(\text{Ar[2p]})3d^2$ and (Ar[2p])4s3d which coupled to give a total angular momentum J of $\frac{1}{2}$ or $\frac{3}{2}$. The MCDF-AL calculations were then performed for each J value separately. Figs 4*a* and 4*b* display the energy level diagrams for $J = \frac{1}{2}$ and $J = \frac{3}{2}$ respectively. The CSF are represented in the default jj coupling scheme. While it might be argued that the valence electrons at least should be represented in LS coupling, it is clear from the energy level diagram that the CSF (leftmost level diagram) are divided according to the core hole: the states with a $2\bar{p}$ hole are separated from the CSF with a 2p hole by at least 0·65 eV in the $J = \frac{3}{2}$ manifold, and by at least 1·98 eV in the $J = \frac{1}{2}$ manifold. The 4s orbital and the 3d orbital are very similar in energy, but the

* The notation (Ar[2p]) indicates the core configuration, i.e. an Ar atom with a hole in the 2p subshell.

ordering of the states is $4s^2 > 4s3d \approx 3d^2$. For the $J = \frac{1}{2}$ manifold, the $|(Ar[2\bar{p}])4s^2\rangle$ CSF is clearly the highest, but for the $J = \frac{3}{2}$ manifold, the $|(Ar[2p])4s^2\rangle$ CSF is nearly degenerate (0·01 eV) with a CSF from the configuration $(Ar[2\bar{p}])4s3d$ with $J = \frac{3}{2}$, and is within 0·12 eV of a CSF from the configuration $(Ar[2\bar{p}])3d^2$. Thus, although there is a strong mixture between $|(Ar[2p_J])4s^2\rangle$ and $|(Ar[2p_J])(3d^2\ {}^1S)\rangle$, for $J = \frac{3}{2}$ there is extra mixing, which spreads the $(Ar[2p])4s^2$ configuration further over the ASF. The effects of the near degeneracy are altered by the inclusion of higher-order effects. There is a shift of about 0·1 eV downwards of the $2\bar{p}$ hole states relative to the 2p hole states, which alters the degree of mixing of the $(Ar[2p])4s^2$ CSF in the ASF. With the Dirac–Coulomb Hamiltonian only, the largest weight of the $(Ar[2p])4s^2$ configuration is 78% for $J = \frac{1}{2}$ and 34% for $J = \frac{3}{2}$. When the higher-order terms are included, the $J = \frac{1}{2}$ weight changes negligibly, but the $J = \frac{3}{2}$ weight is altered to 41%. The ratio of the $L_3 : L_2$ Auger diagram lines is about 1 : 1, as found experimentally. The strong mixing also gives rise to the intense satellite structure on the low energy side of the diagram lines, by population of a series of initial states of the Auger process.

5. Conclusions

In summary, relativistic effects are clearly important in the outer shells of heavy elements, and often have importance where there are near-degeneracies, even in light atoms. For atomic structure calculations, the MCDF method offers an effective way of including relativistic effects in structure calculations, although in many cases, perturbation methods are adequate. Molecular calculations using the Dirac equation are still in their infancy, but progress is being made towards their implementation (see Grant 1986 for a discussion).

References

Banna, M. S. (1985). *J. Chem. Educ.* **62**, 197.
Breuckmann, B. (1978). Ph.D. Thesis, Universität Freiburg.
Desclaux, J.-P. (1975). *Comput. Phys. Commun.* **9**, 31.
Froese Fischer, C. (1977). 'The Hartree–Fock Method for Atoms' (Wiley: New York).
Grant, I. P. (1986). *Aust. J. Phys.* **39**, 649.
Grant, I. P., McKenzie, B. J., Norrington, P. H., Mayers, D. F., and Pyper, N. C. (1980). *Comput. Phys. Commun.* **21**, 207.
McKelvey, D. R. (1983). *J. Chem. Educ.* **60**, 112.
McKenzie, B. J., Grant, I. P., and Norrington, P. H. (1980). *Comput. Phys. Commun.* **21**, 233.
Malli, G. (Ed.) (1983). 'Relativistic Effects in Atoms, Molecules and Solids', NATO ASI Series B, Vol. 87 (Plenum: New York).
Pitzer, K. S. (1979). *Acc. Chem. Res.* **12**, 271.
Pyykkö, P. (1978). *Adv. Quantum Chem.* **11**, 353.
Pyykkö, P., and Desclaux, J.-P. (1979). *Acc. Chem. Res.* **12**, 276.
Rose, S. J., Grant, I. P., and Pyper, N. C. (1978). *J. Phys.* B **11**, 1171.
Weber, W., Chen, M. H., Dyall, K. G., Huster, R., Menzel, W., and Mehlhorn, W. (1983). *In* 'Abstracts of the XIII International Conference on the Physics of Electronic and Atomic Collisions' (North-Holland: Amsterdam).
Weitsman, J., and Hagelstein, P. L. (1986). *J. Phys.* B **19**, L59.

Manuscript received 24 April, accepted 24 June 1986